CERN-PH-TH/2005-050
FERMILAB-PUB-05-050-T

arXiv:hep-ph/0504015 v1 3 Apr 2005

Super-NOνA: a long-baseline neutrino experiment with two off-axis detectors

Olga Mena Requejo[1], Sergio Palomares-Ruiz[2] and Silvia Pascoli[3]
[1] *Theoretical Physics Department, Fermi National Accelerator Laboratory, Batavia, IL 60510-0500, USA*
[2] *Department of Physics and Astronomy, Vanderbilt University, Nashville, TN 37235, USA*
[3] *Physics Department, Theory Division, CERN, CH-1211 Geneva 23, Switzerland*
omena@fnal.gov, sergio.palomares-ruiz@vanderbilt.edu, Silvia.Pascoli@cern.ch

Establishing the neutrino mass hierarchy is one of the fundamental questions that will have to be addressed in the next future. Its determination could be obtained with long-baseline experiments but typically suffers from degeneracies with other neutrino parameters. We consider here the NOνA experiment configuration and propose to place a second off-axis detector, with a shorter baseline, such that, by exploiting matter effects, the type of neutrino mass hierarchy could be determined with only the neutrino run. We show that the determination of this parameter is free of degeneracies, provided the ratio L/E, where L the baseline and E is the neutrino energy, is the same for both detectors.

PACS numbers: 14.60.Pq

I. INTRODUCTION

During the last several years the progress in the studies of neutrino oscillations has been remarkable. The experiments with solar [1, 2, 3, 4, 5, 6], atmospheric [7], reactor [8] and recently also long-baseline accelerator [9] neutrinos have provided compelling evidence for the existence of neutrino oscillations driven by non-zero neutrino masses and neutrino mixing. We know that there are two large (θ_{12} and θ_{23}) and one small (θ_{13}) angles, and at least two mass square differences [1], $\Delta m^2_{ji} \equiv m^2_j - m^2_i$, with $m_{j,i}$ the neutrino masses, one associated to atmospheric neutrino oscillations (Δm^2_{31}) and one to solar ones (Δm^2_{21}). The angles θ_{12} and θ_{23} represent the neutrino mixing angles responsible for the solar and the dominant atmospheric neutrino oscillations, while θ_{13} is the angle limited by the data from the CHOOZ and Palo Verde experiments [13, 14].

Stronger evidences of neutrino oscillations are provided by the new Super-Kamiokande data on the L/E dependence of multi-GeV μ-like atmospheric neutrino events [15], L being the distance traveled by neutrinos and E the neutrino energy, and by the new more precise spectrum data of the KamLAND [16] and K2K experiments [9]. For the first time these data exhibit directly, not only a deficit with respect to the expected signal, but also the effects of the oscillatory dependence on L/E of the probabilities of neutrino oscillations in vacuum [17]. We begin to actually "see" the oscillatory behavior of neutrino propagation.

The Super-Kamiokande and K2K data are best described in terms of dominant $\nu_\mu \to \nu_\tau$ ($\bar\nu_\mu \to \bar\nu_\tau$) vacuum oscillations. The best-fit values explaining the Super-Kamiokande data [7] are $|\Delta m^2_{31}| = 2.1 \times 10^{-3}$ eV^2, $\sin^2 2\theta_{23} = 1.0$, whereas those for the K2K data [9] are $|\Delta m^2_{31}| = 2.8 \times 10^{-3}$ eV^2, $\sin^2 2\theta_{23} = 1.0$. The 90% C.L. allowed ranges of the atmospheric neutrino oscillation parameters obtained by the Super-Kamiokande experiment read [7]:

$$|\Delta m^2_{31}| = (1.5 - 3.4) \times 10^{-3}\text{eV}^2, \qquad \sin^2 2\theta_{23} \geq 0.92. \tag{1.1}$$

The sign of Δm^2_{31} and of $\cos 2\theta_{23}$, when $\sin^2 2\theta_{23} \neq 1.0$, cannot be determined with the existing data. For the mass square difference, the two possibilities, $\Delta m^2_{31} > 0$ or $\Delta m^2_{31} < 0$, correspond to two different types of neutrino mass ordering: normal hierarchy (NH), $m_1 < m_2 < m_3$ ($\Delta m^2_{31} > 0$), and inverted hierarchy (IH), $m_3 < m_1 < m_2$ ($\Delta m^2_{31} < 0$). The fact that the sign of $\cos 2\theta_{23}$ is not determined when $\sin^2 2\theta_{23} \neq 1.0$ implies that the octant where θ_{23} lies is not known.

In addition, the combined 2-neutrino oscillation analysis of the solar neutrino data, including the results from the complete salt phase of the Sudbury Neutrino Observatory (SNO) experiment [6], and the recent KamLAND 766.3

[1] We restrict ourselves to a three-family neutrino scenario analysis. The unconfirmed LSND signal [10] cannot be explained in terms of neutrino oscillations within this scenario, but might require additional light sterile neutrinos or more exotic explanations (see e.g. Ref. [11]). The ongoing MiniBooNE experiment [12] is expected to explore all of the LSND oscillation parameter space [10].

ton-year spectrum data [16] shows that the solar neutrino oscillation parameters lie in the low-LMA (Large Mixing Angle) region, with the best fit value at [6]

$$\Delta m^2_{21} = 8.0 \times 10^{-5}\ \mathrm{eV}^2, \quad \sin^2\theta_{12} = 0.31. \tag{1.2}$$

In a 3-neutrino oscillation framework, a combined analysis of the solar, atmospheric, reactor and long-baseline neutrino data gives [18] (see also Ref. [19]):

$$\sin^2\theta_{13} < 0.041, \quad 3\sigma\ \mathrm{C.L.} \tag{1.3}$$

As we know that neutrinos do oscillate, there are very important questions that will have to be addressed in future experiments. Besides the more accurate determination of the leading neutrino oscillation parameters that will be achieved by the MINOS [20], OPERA [21] and ICARUS [22] experiments and future atmospheric and solar neutrino detectors [23], one of the most important tasks in the next future will be the determination of the (1,3) sector of the lepton mixing matrix, the Pontecorvo–Maki–Nakagawa–Sakata (PMNS) neutrino matrix [24]. A complete determination of this sector entails the measurement of a non-zero θ_{13}, which will open the door to the experimental measurement of the CP– (or T–) violating phase, δ, and to establishing the type of neutrino mass spectrum. This mixing angle controls the $\nu_\mu \to \nu_e$ and $\bar{\nu}_\mu \to \bar{\nu}_e$ conversions in long-baseline experiments and in the widely discussed very long-baseline neutrino oscillation experiments at neutrino factories [25, 26]. More recently, β-beams experiments, exploiting neutrinos from boosted-ion decays [27, 28, 29], with an improved experimental setup have been shown to achieve sensitivities to leptonic CP–violation and to the sign of the atmospheric mass difference competitive with those at neutrino factories [30]. The mixing angle θ_{13} also controls the Earth matter effects in multi-GeV atmospheric [31, 32, 33, 34, 35] and in supernova [36] neutrino oscillations. Finally, the magnitude of the T-violating and CP–violating terms in neutrino oscillation probabilities is directly proportional to $\sin\theta_{13}$ [37]. Therefore the determination of the magnitude of θ_{13} is crucial for the future searches for matter effects and CP–violation in the lepton sector at neutrino oscillation experiments.

The measurement of, or a stronger limit on, the mixing angle θ_{13} in the near future is going to be achieved by reactor [38] and long-baseline [20, 21, 22, 39, 40, 41] neutrino experiments. Neutrino reactor experiments, being disappearance experiments, are only sensitive to the value of θ_{13}. Long-baseline neutrino experiments, in addition to having a better sensitivity to θ_{13}, are the only way (in the near future) to search for CP violation, while being able to determine the type of hierarchy at the same time[2]. However, long-baseline neutrino oscillation experiments suffer from degeneracies in the neutrino parameter space [50, 51, 52, 53, 54]. In general, the proposed experiments have a single detector with the beam running in two different modes, neutrinos and antineutrinos. With only one neutrino and one antineutrino run, the degeneracies can lead to different CP–violating and CP–conserving sets of parameters explaining the data at the same confidence level. In Ref. [26] it was pointed out that some of the degeneracies could be eliminated with sufficient energy or baseline spectral information. In practice, however, the spectral information has been shown to be not strong enough to resolve degeneracies with a single detector, once that statistical errors and realistic efficiencies and backgrounds are taken into account. In order to resolve the parameter degeneracy, another detector [51, 55, 56, 57, 58] or the combination with another experiment [59, 60, 61, 62, 63, 64, 65] would, thus, be necessary. Recently, new approaches for determining the type of hierarchy have been proposed [66]; they typically exploit other neutrino oscillations channels, such as muon neutrino disappearance, and require very precise neutrino oscillation measurements.

Contrary to the naïve expectation, it has been shown numerically in Ref. [60] and analytically in Ref. [61] that the use of only a neutrino beam could help in resolving the type of hierarchy when two different long-baseline experiments are combined under certain conditions.

Differently from this approach, we present here a scenario with only one experiment, which runs in the neutrino mode and uses two detectors at different distances and different off-axis angles. It is well known that off-axis neutrino beams have a very narrow neutrino spectra, and that the peak energy can be tuned by just moving the detector with respect to the main beam axis. We notice that an off-axis beam can be obtained by either displacing the detector a few km away from the location of an on-axis surface detector, or by placing it on the vertical of the beam-line but at a much shorter distance. In such a way, a single beam could do the job of two beams with different energies.

---

[2] The same capabilities with better sensitivity could be achieved by neutrino factories [25, 26]. Information on the type of neutrino mass hierarchy might be obtained in future atmospheric neutrino experiments [32, 33, 34, 35]. If neutrino are Majorana particles, next generation neutrinoless double $\beta-$decay experiments could establish the type of neutrino mass spectrum [42] (see also Refs. [43, 44, 45, 46]) and, possibly, might provide some information on the presence of CP–violation in the lepton sector due to Majorana CP–violating phases [47] (see also Refs. [44, 46, 48, 49]).

We study the use of two off-axis detectors in combination with the NuMI beam so that the type of mass spectrum could be determined free of other degeneracies, if θ_{13} is not very small. We will consider, for one of them, the location which is the most likely for the NOνA configuration[3] ($L = 810$ km and $E = 2.3$ GeV) and show different possibilities for the baseline of the other detector in order to make the measurement of $sign(\Delta m^2_{31})$ feasible with only the neutrino beam. We name this improved experimental setup Super-NOνA [67]. Following the line of thought of Ref. [61], we will show that a configuration with the same vacuum oscillation phase, i. e. same L/E for both detectors, is specially sensitive to matter effects. For such an experimental setup the sensitivity to $sign(\Delta m^2_{31})$ would be enhanced as the difference in baseline lengths grows. This configuration also has the advantage of requiring only one experiment and of reducing the error due to systematic uncertainties from the beam. In addition, we will show that such a measurement is free of degeneracies, which provides the full power of this method. We start by presenting the general formalism in Sec. II. In Sec. III we describe the experimental setup. We explain in Sec. IV the method to extract the type of neutrino mass spectrum free of degeneracies by using this special configuration and we show how the sensitivity changes for different values of $|\Delta m^2_{31}|$. Finally, in Sec. V, we make our final remarks. In Appendix A we present the computed charged-current (CC) neutrino event rates for a particular choice of parameters.

II. FORMALISM

We consider the probability of $\overset{(-)}{\nu}_\mu \to \overset{(-)}{\nu}_e$ oscillation, $P\left(\overset{(-)}{\nu}_\mu \to \overset{(-)}{\nu}_e; L\right) \equiv \overset{(-)}{P}(L)$, in the context of three-neutrino mixing. For neutrino energies $E \gtrsim 1$ GeV, θ_{13} within the present bounds [18, 19], and baselines $L \lesssim 1000$ km [53] [4], the oscillation probability $\overset{(-)}{P}(L)$ can be safely approximated by expanding in the small parameters θ_{13}, Δ_{12}/Δ_{13}, Δ_{12}/A and $\Delta_{12}L$, where $\Delta_{12} \equiv \Delta m^2_{21}/(2E)$ and $\Delta_{13} \equiv \Delta m^2_{31}/(2E)$ [26] (see also Ref. [68]):

$$\begin{aligned}\overset{(-)}{P}(L) \simeq\ & \sin^2\theta_{23}\,\sin^2 2\theta_{13}\left(\frac{\Delta_{13}}{A\mp\Delta_{13}}\right)^2 \sin^2\left(\frac{(A\mp\Delta_{13})L}{2}\right) \\ & + \cos\theta_{13}\sin 2\theta_{13}\sin 2\theta_{23}\sin 2\theta_{12}\ \frac{\Delta_{12}}{A}\frac{\Delta_{13}}{A\mp\Delta_{13}}\ \sin\left(\frac{AL}{2}\right)\sin\left(\frac{(A\mp\Delta_{13})L}{2}\right)\cos\left(\frac{\Delta_{13}L}{2}\mp\delta\right) \\ & + \cos^2\theta_{23}\sin^2 2\theta_{12}\left(\frac{\Delta_{12}}{A}\right)^2\sin^2\left(\frac{AL}{2}\right),\end{aligned} \tag{2.1}$$

where L is the baseline. We use the constant density approximation for the index of refraction in matter A, defined as $A \equiv \sqrt{2}G_F\bar{n}_e(L)$, with $\bar{n}_e(L)$ the average electron number density, defined by $\bar{n}_e(L) = 1/L\int_0^L n_e(L')dL'$. Here $n_e(L)$ is the electron number density along the baseline.

As is well known [52], the CP trajectory in bi–probability plots of neutrino and antineutrino conversion at the same baseline, is elliptic under the assumption of mass hierarchy and of adiabaticity. The ellipses obtained for each of the two hierarchies, and for different values of δ, θ_{13} and of θ_{23}, intersect in points that correspond to 2–, 4–, and 8–fold degeneracies [50, 51, 52, 53, 54]. It follows that even a precise determination of a point in the P–$\bar{P}$ plane can result in different sets of CP–conserving and CP–violating parameters (δ, θ_{13}, θ_{23}, $sign(\Delta m^2_{31})$), all of which reproduce the observations. The allowed regions in the P–$\bar{P}$ plane obtained by varying the values of θ_{13} and δ within their ranges describe wide "pencils". The "pencils" for the cases of normal and inverted hierarchy have different slopes and overlap for a large fraction. This indicates that, generically, a measurement of the probability of conversion for neutrinos and antineutrinos cannot uniquely determine the type of hierarchy in a single experiment. In order to resolve such degeneracy, various strategies have been proposed: combined analysis of the data from different super-beam experiments, or of the data from super-beam facilities and neutrino factories (or β-beams) [30, 59, 60, 61, 62, 63], the use of additional information from atmospheric neutrino data [64], and experimental setups with clusters of detectors [51, 55, 56, 58].

It has been pointed out that considering the probabilities of neutrino oscillations only, at two different baselines and energies, can resolve the type of hierarchy [60, 61]. In the case of bi–probability plots of neutrino–neutrino conversions at different baselines, the CP–trajectory is elliptic too. Again, the allowed regions in these bi–probability plots form two "pencils", which grow in width away from the origin, each of them associated with one type of mass spectrum. The overlap of the two "pencils", which signals the presence of a degeneracy of the type of hierarchy with other parameters, is controlled by the slope and the width of the "pencils". From Eq. (2.1) one can see that the ratio of the slopes of the central axes of these two "pencils" in the $P_{\rm F}$–$P_{\rm N}$ plane, where $P_{\rm F}$ ($P_{\rm N}$) is the neutrino conversion

[3] This values correspond to the already old NOνA proposal [40]. For the recent revised proposal see Ref. [41].

[4] For $E \gtrsim 0.6$ GeV we have checked that the analytical expansion is accurate for $L < 500$ km within the present bounds of θ_{13} and $\Delta m^2_{21}/\Delta m^2_{31}$.

probability at the far (near) detector, is given by [61]

$$\frac{\alpha_+}{\alpha_-} = \frac{\left(\frac{\Delta_{13,\mathrm{N}}}{A_\mathrm{N}-\Delta_{13,\mathrm{N}}}\right)^2 \sin^2\left(\frac{(A_\mathrm{N}-\Delta_{13,\mathrm{N}})L_\mathrm{N}}{2}\right)\left(\frac{\Delta_{13,\mathrm{F}}}{A_\mathrm{F}+\Delta_{13,\mathrm{F}}}\right)^2 \sin^2\left(\frac{(A_\mathrm{F}+\Delta_{13,\mathrm{F}})L_\mathrm{F}}{2}\right)}{\left(\frac{\Delta_{13,\mathrm{F}}}{A_\mathrm{F}-\Delta_{13,\mathrm{F}}}\right)^2 \sin^2\left(\frac{(A_\mathrm{F}-\Delta_{13,\mathrm{F}})L_\mathrm{F}}{2}\right)\left(\frac{\Delta_{13,\mathrm{N}}}{A_\mathrm{N}+\Delta_{13,\mathrm{N}}}\right)^2 \sin^2\left(\frac{(A_\mathrm{N}+\Delta_{13,N})L_\mathrm{N}}{2}\right)} \tag{2.2}$$

where α_+ and α_- are the slopes for normal and inverted hierarchy, respectively; $\Delta_{13,\mathrm{F(N)}}$, $A_{\mathrm{F(N)}}$ and $L_{\mathrm{F(N)}}$ are the values of Δ_{13}, A and L for the far (near) detector. Note that although we are using the constant density approximation, A_F and A_N are different because the average density depends on the baseline. Using the fact that matter effects are small ($A \ll \Delta_{13}$), we can perform a perturbative expansion, which up to first order gives this ratio of slopes as

$$\frac{\alpha_+}{\alpha_-} \simeq 1 + 2\,A_\mathrm{N}L_\mathrm{N}\left(\frac{1}{(\Delta_{13,\mathrm{N}}L_\mathrm{N}/2)} - \frac{1}{\tan(\Delta_{13,\mathrm{N}}L_\mathrm{N}/2)}\right) - 2\,A_\mathrm{F}L_\mathrm{F}\left(\frac{1}{(\Delta_{13,\mathrm{F}}L_\mathrm{F}/2)} - \frac{1}{\tan(\Delta_{13,\mathrm{F}}L_\mathrm{F}/2)}\right). \tag{2.3}$$

For the case of L/E constant, noting that $1/x - 1/\tan x$ is a monotonically increasing function, we conclude that the smaller the chosen energy, the larger the ratio of slopes. This ratio increases also for certain configurations with different L/E [61]. Another very important feature is the width, which is very small for equal L/E, but grows rapidly when this is not the case [61]. Hence, even when the separation between the central axes of the two regions is substantial, unless the ratio L/E is kept close to constant, the ellipses overlap, making the discrimination of $sign(\Delta m^2_{31})$ challenging. As was shown in Ref. [61], away from the L/E-constant case, the choice $L_\mathrm{F}/E_\mathrm{F} > L_\mathrm{N}/E_\mathrm{N}$ is preferred. Otherwise, no matter how accurate the experiment is, the discrimination of the type of neutrino mass hierarchy free of degeneracies will not be possible. As a matter of fact, this is precisely what will happen when combining NOνA and T2K experiments, for which $L_{\mathrm{NO}\nu\mathrm{A}}/E_{\mathrm{NO}\nu\mathrm{A}} = 352\,\mathrm{km/GeV} < 421\,\mathrm{km/GeV} = L_{\mathrm{T2K}}/E_{\mathrm{T2K}}$[5]. In this case, a joint analysis of these two experiments does not present any interesting synergy effects and just accounts for adding in statistics [60].

Thus, we will consider the case of L/E constant and show how, by adding another detector to the already proposed NOνA experimental setup, the measurement of the $sign(\Delta m^2_{31})$ is possible free of degeneracies from other parameters.

III. EXPERIMENTAL SETUP

As was pointed out in the previous section, we consider here only one experiment by using the same beam but having two detectors. In order to maximize the sensitivity to the type of hierarchy, we propose a configuration in which the neutrino conversion takes place predominantly at the same L/E at the two locations. In such a way, matter effects can be factored out and the type of neutrino mass hierarchy can be determined (if θ_{13} is large enough), free of degeneracies from other parameters of the neutrino mixing matrix.

In order to have the same L/E for both detectors we would need a very well peaked spectrum at both sites. This can be achieved by placing the detectors off the central axis of the beam. As is well known, most of the neutrinos in a conventional neutrino beam are produced in two-body decays $\pi^\pm \to \mu^\pm + \overset{(-)}{\nu}_\mu$. The energy and flux of these neutrinos is determined by the decay angle θ [69]:

$$E = \frac{0.43\,E_\pi}{1+\gamma^2\,\theta^2}, \tag{3.1}$$

$$\Phi = \left(\frac{2\,\gamma}{1+\gamma^2\,\theta^2}\right)^2 \frac{1}{4\pi L^2}\ , \tag{3.2}$$

where γ is the Lorentz factor of the pion, θ is the angle between the pion and the neutrino directions, and L is the distance between the decay point and the detector. A neutrino beam with narrow energy spectrum can be produced by placing the detector off-axis, i. e., at some angle with respect to the forward direction $\theta_\mathrm{beam} = 0$. By using off-axis beams, one manages a kinematic suppression of the high energy neutrino components, whereas the low energy flux is kept approximately the same as that of the on-axis beams. The neutrino spectrum is very narrow in energy and peaked at lower energies with respect to the on-axis one. The suppression of the high-energy tail of the spectrum

[5] This corresponds to the configuration with an off-axis angle of 2° (OA2^o) for T2K [39].

greatly reduces the backgrounds due to neutral-current interactions and τ production. Since the neutrino flux is nearly monochromatic, the off-axis technique allows a discrimination between the peaked ν_e oscillation signal and the intrinsic ν_e background which has a broad energy spectrum. An efficient reduction of the intrinsic background can therefore be achieved [69].

The off-axis angle and baseline for each detector must be chosen in such a way that we have the same L/E at both sites. From Eqs. (3.1) and (3.2) we see that the flux scales as $\Phi \sim (E/L)^2$; so for this special configuration the flux at the near detector is of the same order as that at the far detector (see Appendix A). For the far detector we will use the configuration proposed for the NOνA experiment and we will suggest to place another detector of the same characteristics at a closer distance from the source.

From geometrical considerations, and using the fact that the Earth is curved, a detector located on the Earth surface, on the vertical line of the central axis of the beam, is off-axis by a small angle, $\theta_{\rm min}$. This is the minimum off-axis angle at a given distance for a given beam configuration, which for $L_{\rm F,N,on-axis} \ll R$, reads

$$(\theta_{\rm min})_{\rm F,N} \simeq \frac{L_{\rm on-axis} - L_{\rm F,N}}{2R}, \tag{3.3}$$

where $L_{\rm on-axis} = 735$ km is the baseline for the on-axis detector (MINOS), R is the Earth radius, and we have neglected terms of order $(L_{\rm F,N,on-axis}/R)^3$. A different (larger) off-axis angle at the same distance can be achieved by placing the detector slightly outside the vertical of the beam. We present here the possible locations for the near detector.

It turns out that the peak energy in the ν_μ CC neutrino event spectrum is well fitted by the parametrization [70]

$$E_{\rm peak} = \frac{1900}{(\theta + 16)^2}\ {\rm GeV}, \tag{3.4}$$

with θ the off-axis angle in units of mrad. Then one has to solve for the detector locations that have a constant ratio of $L/E \simeq 810\,{\rm km}/2.3\,{\rm GeV} = 352\,{\rm km/GeV}$. From Eq. (3.4), it is clear that we can write θ as a function of the baseline L for constant L/E, which reads

$$\theta(L) = 16\left(51\left(\frac{\rm km}{L}\right)^{1/2}\left(\frac{L/E}{352\,{\rm km/GeV}}\right)^{1/2} - 1\right){\rm mrad}. \tag{3.5}$$

Once the possible values of the off-axis angle θ and the associate peak energy $E_{\rm peak}$ are determined for a given distance L, it is absolutely necessary to check whether or not the geometry of the Earth and the NuMI beamline allow the different configurations to be a reality [70]. From Eqs. (3.3) and (3.5), the condition for this to be possible is $\theta(L) > \theta_{\rm min}$. In particular, there are no sites between 300 and 400 km which give an L/E ratio of 352 km/GeV. We have explored four possible detector locations: 200, 434, 500 and 600 km [70]. Here we only present the results for the detector locations at 200 km and 434 km, since the distinction of the neutrino mass hierarchy is easier for shorter baselines, as we will show below. These configurations correspond to off-axis angles of 42.2 and 23.6 mrad, respectively. We have used the neutrino and antineutrino fluxes available at different off-axis configurations at the NOνA far site (810 km) and obtained the fluxes at the short baselines by a simple rescaling of the fluxes at the far distance[6].

In the old proposal [40], the NOνA far detector at 810 km is a 50 kton tracking calorimeter, and the efficiency for its accepting a ν_e event from $\nu_\mu \to \nu_e$ oscillations is approximately 21%. We have explored here the possibility of using a 50 kton liquid argon TPC detector [72], for which the efficiency to identify ν_e CC interactions is 90% (i. e., basically perfect efficiency) and that the background is dominated by the intrinsic ν_e and $\bar{\nu}_e$ components of the beam. The high detection efficiency of a liquid argon detector makes its statistics equivalent to that of a conventional detector, with the beam power upgraded with the proton driver. In addition, the physics potential of these detectors is remarkable, as supernova neutrino detectors, for proton decay searches[7] and for studies of neutrinoless double beta decay (see Ref. [72] and references therein).

We have assumed that the number of protons on target per year is 3.7×10^{20} [40] (18.5×10^{20} pot/yr with the Proton Driver) and five years of neutrino running. The revised NOνA proposal [41] suggests a number of protons on target per year which has been upgraded to 6.5×10^{20} (25×10^{20} with a Proton Driver) and a 30 kton detector with 24% efficiency.

---

[6] The short-baseline fluxes at 200 km can be easily obtained from the fluxes at 735 km and 30 km off axis [71]. The fluxes at 434 km have been computed from the ones at 810 km and 18 km off-axis.

[7] If protons decay primarily into kaons ($p \to K^+ + \nu$), the detection efficiency in water-Čerenkov detectors is relatively low, for kaons at these energies are below threshold.

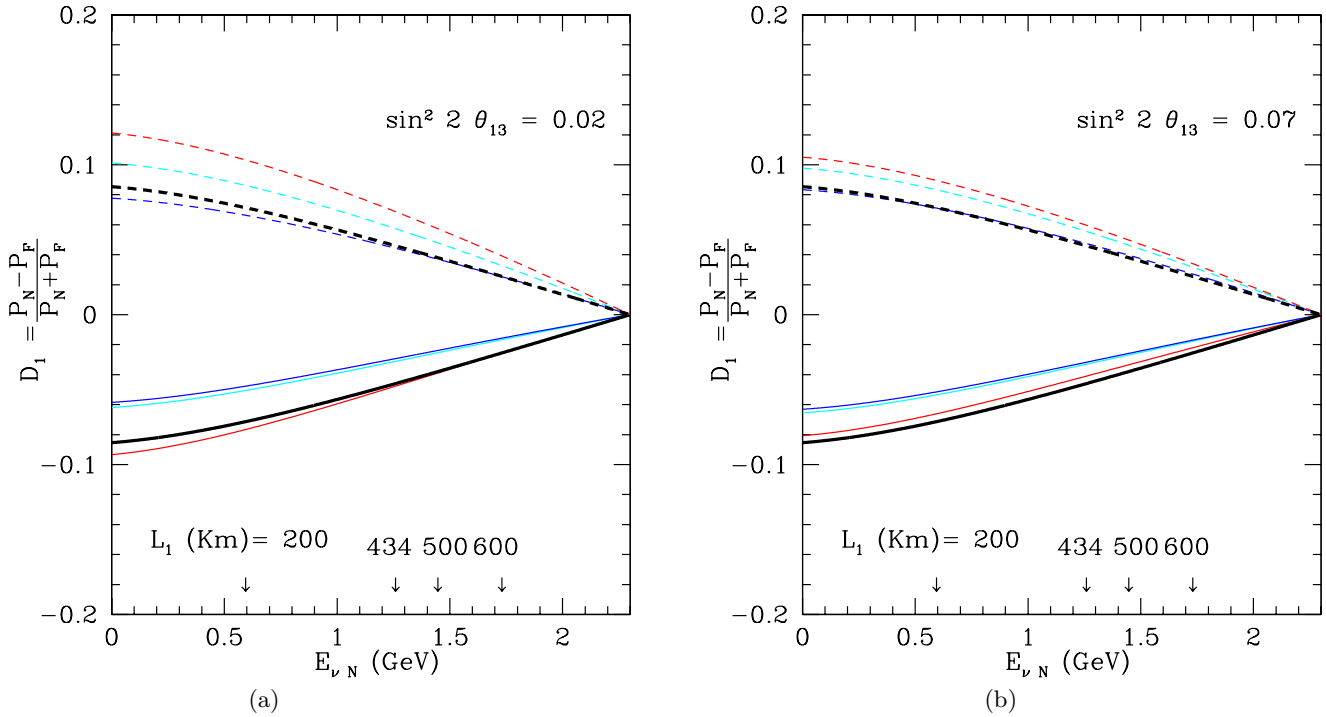

FIG. 1: *(a) Approximate probability difference, Eq. (4.2), as a function of the neutrino energy for normal (black thick solid curve) and inverted hierarchies (dashed thick black curve) for* $\sin^2\theta_{13} = 0.02$. *We also depict the exact computation of the probability difference for the two hierarchies and different values of* δ. *From smaller to larger values of* $|\mathcal{D}|$: $\delta = \frac{\pi}{2}$ *(blue), 0 (cyan) and* $\frac{3\pi}{2}$ *(red) (color online). In the x-axis we specify the distances that we have explored as possible locations for the near detector, related to the neutrino energy by* $L_{\rm N} = E_{\rm N} L_{\rm F}/E_{\rm F}$. *In this study we present the results for* $L_{\rm N} = 200, 434$ *km. (b) Same as (a) but for* $\sin^2 2\theta_{13} = 0.07$.

A. Oscillated statistics

For a given value of the oscillation parameters, we have computed the expected number of electron events, N_ℓ detected at the possible locations $\ell = {\rm N}, {\rm F}$ (near/far sites). The observable that we exploit, N_ℓ, reads

$$N_{\ell,\pm} = \int_{E_{\rm min}}^{E_{\rm max}} \Phi_{\ell,\nu}(E_\nu, L)\, \sigma_\nu(E_\nu)\, P_\nu(E_\nu, L, \theta_{13}, \delta, \Delta m^2_{31}, \alpha)\, dE_\nu \tag{3.6}$$

where the sign $+(-)$ applies for the normal (inverted) hierarchies and α is the set of remaining oscillation parameters: θ_{23}, θ_{12}, Δm^2_{21} and the matter parameter A (which depend on the baseline under consideration), which are taken to be known; $\Phi_{\ell,\nu}$ denotes the neutrino flux and σ_ν the cross sections. The neutrino fluxes are thus integrated over a narrow energy window, where $E_{\rm min}$ and $E_{\rm max}$ refer to the lower and upper energy limits respectively.

For our analysis, unless otherwise stated, we will use a representative $|\Delta m^2_{31}| = 2.4 \times 10^{-3}$ eV^2, which lies within the best-fit values for the Super-Kamiokande [7] and K2K [9] experiments. However, we will also show how the results change for different values of this parameter. For the rest of the parameters, θ_{23}, Δm^2_{21} and θ_{12}, we will use the best fit values quoted in the introduction. We show in Appendix A the expected number of signal and background events at the far location ($L = 810$ km) and at two of the possible near locations ($L = 200$ km and $L = 434$ km) for both hierarchies and four central values of the CP phase $\delta = 0, \frac{\pi}{2}, \pi, \frac{3\pi}{2}$ and $\sin^2 2\theta_{13} = 0.058$.

IV. MATTER EFFECTS AND THE TYPE OF HIERARCHY

The first task of a long-baseline neutrino experiment should be to measure the small θ_{13} angle of the neutrino mixing matrix. Adding one detector to the experiment would increase the statistics and then the sensitivity to this mixing angle. Here, we will assume that the value of θ_{13} is within the sensitivity of next-generation long-baseline and

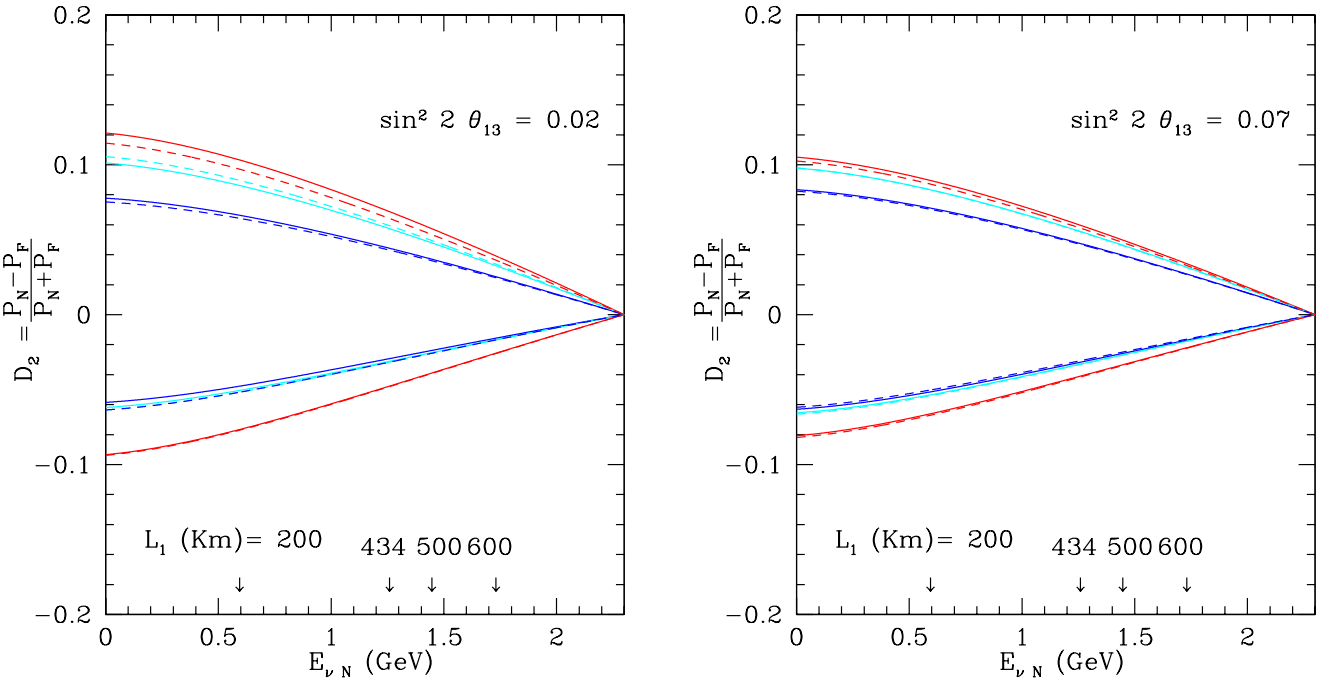

(a) (b)

FIG. 2: *(a) The dashed curves depict the probability difference up to second order in Eq. (4.3), as a function of the neutrino energy for normal (lower curves) and inverted hierarchies (upper curves) for* $\sin^2 2\theta_{13} = 0.02$ *together with the exact computation (solid curves). From smaller to larger values of* $|\mathcal{D}|$*, we plot three different values of* $\delta = \frac{\pi}{2}$ *(blue), 0 (cyan) and* $\frac{3\pi}{2}$ *(red) (color online). In the x-axis we specify the distances that we have explored as possible locations for the near detector, related to the neutrino energy by* $L_{\rm N} = E_{\rm N} L_{\rm F}/E_{\rm F}$*. In this study we present the results for* $L_{\rm N} = 200$ *and* 434 *km. (b) Same as (a) but for* $\sin^2 2\theta_{13} = 0.07$*.*

reactor neutrino experiments. We will focus on the possibility to discriminate the type of neutrino mass ordering and will show that, by considering the experimental setup described above, the improvement with respect to the current NOνA proposal is remarkable. The study of the enhanced sensitivity to the value of θ_{13} and to the CP–violating phase δ for the experimental configuration presented here will be performed elsewhere [73].

In order to study matter effects, we will consider the probability of ν_μ–ν_e oscillations in matter at two different lengths of the baselines, $L_{\rm N}$ (near detector) and $L_{\rm F}$ (far detector). And, as mentioned above, since the sensitivity to the mass hierarchy is optimized for L/E constant, we will consider both baselines so that we keep the same ratio L/E at both detectors. We compute the quantity

$$\mathcal{D} \equiv \frac{P(L_{\rm N}) - P(L_{\rm F})}{P(L_{\rm N}) + P(L_{\rm F})}\,, \tag{4.1}$$

i.e. the normalized difference of the oscillation probabilities computed at the near and far locations. By using the approximate formula Eq. (2.1) and expanding up to first order in matter effects, $AL \ll 1$ and $A \ll \Delta_{13}$, neglecting the solar neutrino mixing parameters and keeping terms of $\mathcal{O}(A\,\theta_{13})$, $\mathcal{D}$ reads

$$\mathcal{D}_1 \simeq \frac{A_{\rm N} L_{\rm N} - A_{\rm F} L_{\rm F}}{2} \left(\frac{1}{(\Delta_{13} L/2)} - \frac{1}{\tan(\Delta_{13} L/2)} \right)\,. \tag{4.2}$$

Let us note that the leading term in Eq. (2.1) is proportional to $\sin^2(\Delta_{13} L/2)$ and cancels out in $\mathcal{D}_1$ because L/E is the same for the near and far detector sites. It is clear from Eq. (4.2) that the probability difference $\mathcal{D}_1$ changes sign if the neutrino mass spectrum is normal or inverted, since it depends on the sign of Δm^2_{31}.

The effects due to the CP–phase δ, as well as those due to the solar neutrino mixing parameters, are subleading for large enough values of $\sin^2\theta_{13} \geq 0.01$, region which is within the range expected to be explored by the NOνA experiment. In Fig. 1 we depict the neutrino energy dependence of the quantity $\mathcal{D}_1$, Eq. (4.2), for the two possible hierarchies and we compare the results with the ones obtained using the exact oscillation probabilities for three

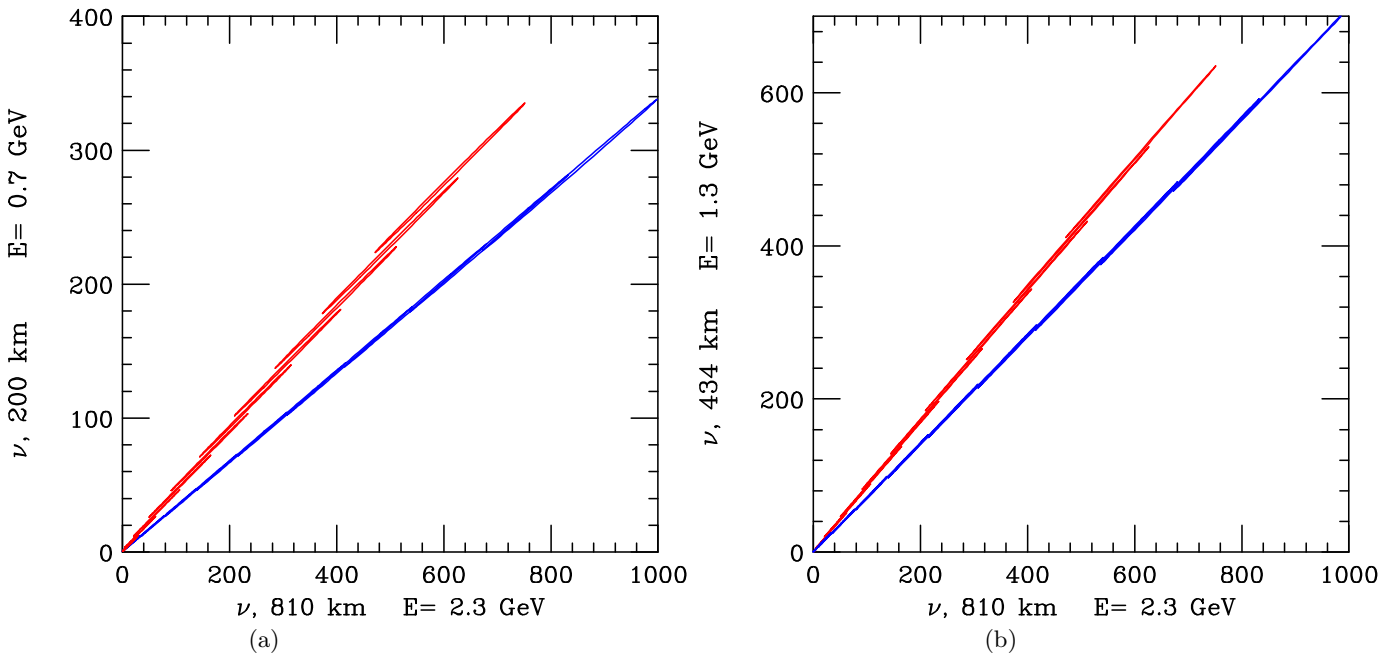

FIG. 3: *(a) Bi–neutrino event ellipses at the short (200 km) and at the far distances (810 km) for normal (lower blue) and inverted (upper red) hierarchies. The experimental setup considered here is* 3.7×10^{20} *protons on target per year, a 50 kton detector with perfect efficiencies at each location and five years of data taking. From bottom up, the ellipses correspond to* $\sin^2 2\theta_{13} = 0.0003, 0.0004, 0.006, 0.008, 0.001, 0.005, 0.01, 0.02, 0.03, 0.04, 0.06, 0.07, 0.095$ *and* 0.11. *(b) Same as (a) but with the near detector located at 434 km.*

different values of the CP–phase $\delta = 0, \frac{\pi}{2}, \frac{3\pi}{2}$. We show our results for two different values of $\sin^2 2\theta_{13} = 0.02$, close to the sensitivity limit for the NOνA experiment and $\sin^2 2\theta_{13} = 0.07$, close to the present upper bound, Eq. (1.3).

For large enough values of $\sin^2 2\theta_{13}$, the contribution of CP effects to $\mathcal{D}_1$ is never larger than 20–30% (see Fig. 1). It can be shown that, at leading order, the second term of the r.h.s. of Eq. (2.1), which controls the CP–violating effects, depends only on L/E. Therefore, in the normalized difference $\mathcal{D}$, the leading CP–violating contribution cancels out and CP–violating effects can be treated as a perturbation to the dominant contribution from matter effects.

The expression for $\mathcal{D}$ with terms up to $\mathcal{O}(A\,\Delta_{12}/\Delta_{13})$, $\mathcal{O}(A\,\theta_{13}^2)$ and $\mathcal{O}(A^2)$ reads[8]:

$$\mathcal{D}_2 \;\simeq\; \mathcal{D}_1 \left(1 - \frac{\Delta_{12}}{\Delta_{13}} \frac{\cos\theta_{13}}{\tan\theta_{23}} \frac{\sin 2\theta_{12}}{\sin 2\theta_{13}} \frac{\Delta_{13} L/2}{\sin(\Delta_{13} L/2)} \cos\left(\delta + \Delta_{13} L/2\right) - \frac{1}{2} \sin^2 2\theta_{13}\right)$$
$$+ \frac{1}{2} \frac{A_{\rm N}^2 L_{\rm N}^2 - A_{\rm F}^2 L_{\rm F}^2}{4} \left(\frac{1}{(\Delta_{13} L/2)^2} - \frac{1}{\sin^2\left(\Delta_{13} L/2\right)}\right) \;, \tag{4.3}$$

where the correction due to the CP–phase also changes sign with the hierarchy type. For instance, for normal hierarchy, the correction to $\mathcal{D}_1$ due to the first term in the r.h.s. of Eq. (4.3) will increase $|\mathcal{D}_1|$ if $\pi/2 < \delta + |\Delta_{13}| L/2 < 3\pi/2$ whereas for inverted hierarchy it will decrease $|\mathcal{D}_1|$ if $\pi/2 < \delta - |\Delta_{13}| L/2 < 3\pi/2$. However, the second-order correction due to matter effects does not depend on $sign(\Delta m_{31}^2)$ and it is always negative.

The probability difference up to second order, Eq. (4.3), is depicted in Fig. 2 for the three different values of the CP–phase $\delta = 0, \frac{\pi}{2}, \frac{3\pi}{2}$ and for the two possible hierarchies. We repeat the same exercise as in Fig. 1 and show our results for two different values of θ_{13}: $\sin^2 2\theta_{13} = 0.02$ and $\sin^2 2\theta_{13} = 0.07$.

We have thus shown that, under this special experimental configuration, determining the type of hierarchy requires only establishing whether $\mathcal{D}$ is positive or negative, being this measurement free of other degeneracies; the corrections due to the rest of the neutrino mixing parameters cannot flip this sign. This implies that the determination of the

[8] In order to obtain the term $\mathcal{O}(A\,\theta_{13}^2)$ one has to use the expression for the probability up to $\mathcal{O}(\theta_{13}^3)$ (see Ref. [26]), and not just Eq. (2.1). For large values of θ_{13} this term is of the order of the $\mathcal{O}(A^2)$ contribution.

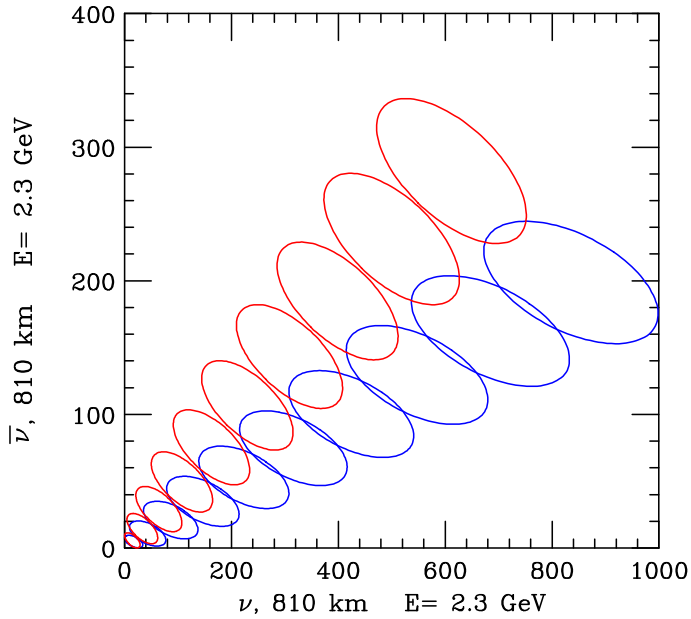

FIG. 4: *Bi–event neutrino–antineutrino ellipses at the far distances (810 km) for normal (lower blue) and inverted (upper red) hierarchies. The experimental setup is the one described in Fig. 3, but considering 5 years of neutrino running and 5 years of antineutrino running. From bottom up, the ellipses correspond to* $\sin^2 2\theta_{13} = 0.001, 0.005, 0.01, 0.02, 0.03, 0.04, 0.06, 0.07, 0.095$ *and* 0.11.

type of hierarchy by using only the neutrino channel with two detectors at different baselines suffers no degeneracies with other parameters. In addition, the requirement of just only the neutrino channel (with two detectors, though) will allow the number of years of data taking (and systematic uncertainties) to be reduced.

In order to illustrate the potential of the combination of two long-baseline detectors operating at the same L/E in extracting $sign(\Delta m^2_{31})$, we show here the neutrino bi–event plots at the far and at the short distance detectors and we compare these results with the neutrino–antineutrino bi–event plots at just one fixed distance. In Fig. 3 we show the neutrino bi–event curves for the two hierarchies at the short and at the far distance, considering two short baselines (200 km and 434 km) and a fixed long-baseline (810 km) for different values of $\sin^2 2\theta_{13}$. As it is clearly seen from these plots, for the case of constant L/E at both detectors, the ellipses collapse to a line and those obtained if the solution is that of $sign(\Delta m^2_{31}) > 0$ no longer overlap with those for $sign(\Delta m^2_{31}) < 0$. Notice also that the slope for the normal hierarchy "pencil" is smaller than that for the inverted hierarchy, because of the larger matter effect for larger baselines (for neutrinos).

If instead we consider the commonly assumed configuration of using a single detector, and running first in the neutrino mode and then in the antineutrino mode, the ellipses overlap for a large fraction of values of the CP–phase δ for every allowed value of $\sin^2 2\theta_{13}$. This makes the determination of $sign(\Delta m^2_{31})$ extremely difficult, i. e., the $sign(\Delta m^2_{31})$-extraction is not free of degeneracies. The former case is depicted in Fig. 4, where we have considered 5 years of neutrino and antineutrino running. Therefore, even with half of the time of data taking, placing two detectors could resolve the type of neutrino mass hierarchy much more easily than the standard approach.

In what follows, we will provide a detailed study of the sensitivity to the $sign(\Delta m^2_{31})$ in the $\sin^2 2\theta_{13}$–δ plane.

In order to compute the sensitivity to the mass hierarchy, as a first approach, we have constructed a measurable integrated asymmetry:

$$A_+ = \frac{\{N/N_o\}_{\rm N} - \{N/N_o\}_{\rm F}}{\{N/N_o\}_{\rm N} + \{N/N_o\}_{\rm F}}\,, \tag{4.4}$$

where N is the number of ν_e induced events in the presence of oscillations in the normal hierarchy scheme and N_o is the expected number of ν_μ charged-current interactions in the absence of oscillations at the near (N) and far (F) detectors. One can compute the equivalent integrated asymmetry assuming an inverted hierarchical scenario, A_-. If Nature has chosen, for instance, a positive value for the atmospheric splitting but the data analysis is performed assuming the opposite sign, the sensitivity to the sign resolution reads

$$\frac{|A_+ - A_-|}{\delta A_+}\,, \tag{4.5}$$

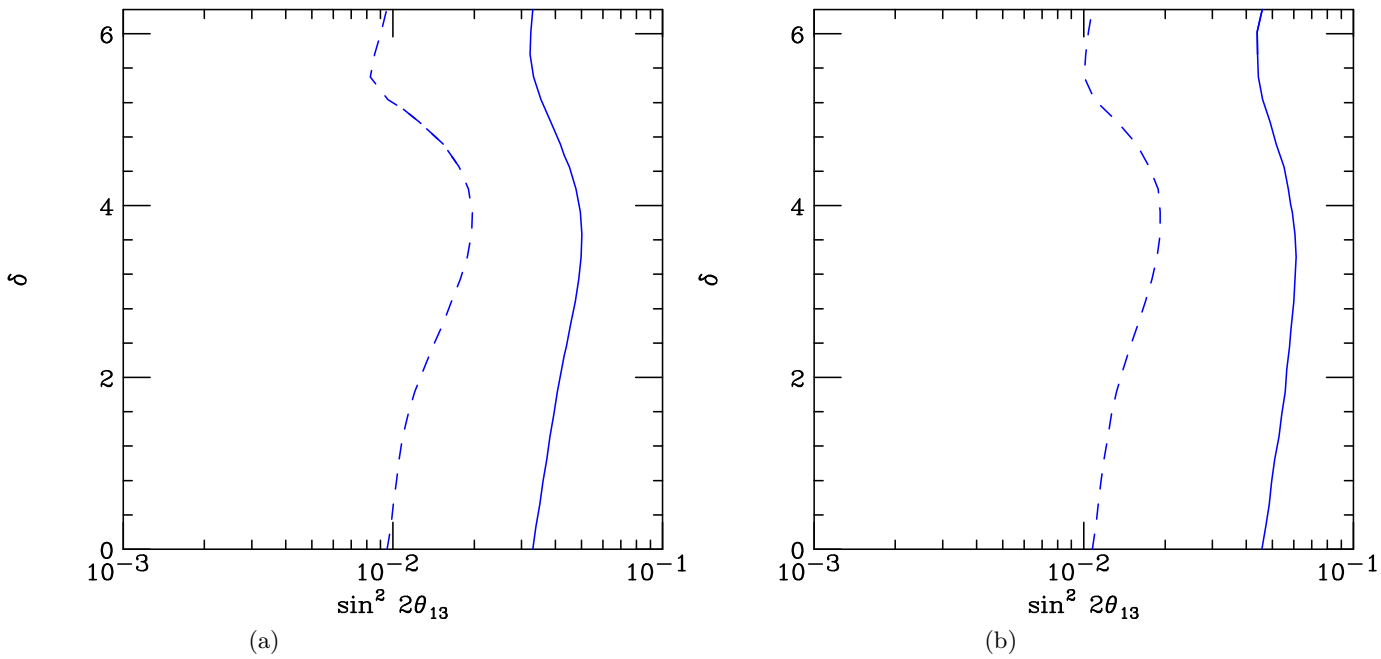

FIG. 5: *(a) Sensitivity to the sign of the atmospheric mass square difference (for $|\Delta m^2_{31}| = 2.4 \times 10^{-3}$ eV^2) as defined in Eq. (4.5), including the systematic errors induced by the uncertainties on the atmospheric mixing parameters and on the matter parameter A, exploiting the data from a short-baseline off-axis detector located at 200 km and from the long-baseline off-axis detector at 810 km. The experimental setup assumed to obtain the solid curves is 3.7×10^{20} protons on target per year, a 50 kton detector with perfect efficiencies at each location and five years of data taking, whereas to get the dashed curves we have added to the former statistics a factor of 5 (proton driver case). (b) Same as (a) but combining the data from the long-baseline with a short-baseline off-axis experiment located at 434 km.*

i. e., the difference between the two asymmetries divided by its error. We have studied the case of statistical errors (adding backgrounds) as well the impact of the uncertainties on the remaining oscillation parameters by computing this *systematic error* on the asymmetry using the standard error propagation method. The errors on the solar parameters can be safely neglected. The errors considered here for the atmospheric mixing parameters Δm^2_{31} and $\sin^2 2\theta_{23}$ are at the level of 5% and 2% respectively [40, 74]. For the matter parameter we take the conservative assumption $\Delta A/A = 5\%$ [75].

We present the 95% C.L. sensitivities to the neutrino mass hierarchy resolution in Fig. 5, where Nature's solution for the neutrino mass spectrum has been chosen to be the normal hierarchy. We have studied both possibilities, normal and inverted hierarchy, as Nature's or "true" solution. We find that the conclusions do not change in a significant way when considering the inverted neutrino mass spectrum.

Two possible combinations of the data at the far, "fixed" NOνA off-axis experiment have been explored: with the data from a near detector located at 200 km and with those from a near detector located at 434 km. All these experiments would exploit the NuMI neutrino beam in an off-axis mode. From the results depicted in Fig. 5, one can observe that the best option for the location of the second, near detector, would be 200 km: the hierarchy could be determined regardless of the value of the CP–phase δ down to values of $\sin^2 2\theta_{13} = 0.05$ or $\sin^2 2\theta_{13} = 0.02$ with the Proton Driver option. For a longer baseline, 434 km, the type of hierarchy can be uniquely determined independently of δ for $\sin^2 2\theta_{13} = 0.06$ and $\sin^2 2\theta_{13} = 0.02$, without and with the Proton Driver, respectively.

For comparison, we consider the study performed in the revised NOνA proposal [41] on the sensitivity to the mass hierarchy. The analysis considers 3 years of running in the neutrino and antineutrino modes, with a 30 kton detector located at a baseline of 820 km and 12 km off-axis. A value of $\Delta m^2_{31} = 2.5 \times 10^{-3}$ eV^2 was chosen. NOνA alone can resolve the sign of Δm^2_{31} at the 95% C.L. for only 10% of the values within the range of the CP–phase δ if $\sin^2 2\theta_{13} = 0.04$. Even if $\sin^2 2\theta_{13} = 0.1$, a value that is very close to the present upper bound, NOνA could uniquely determine the type of hierarchy for only 40% of the values of the CP–phase δ [41]. Even with the Proton Driver, NOνA cannot resolve the sign of the atmospheric mass difference for 80% (40%) of the values of δ if $\sin^2 2\theta_{13} \leq 0.02(0.1)$ [41]. In addition, the possibility of adding a second 50 kton detector at ~ 700 km and 30 km off-axis, is discussed [41, 67]. In this case, the resolution of the mass hierarchy down to $\sin^2 2\theta_{13} = 0.02$ can be accomplished after 12 years of NOνA data plus 6 years with the second detector equally split between neutrinos and antineutrinos and with Proton

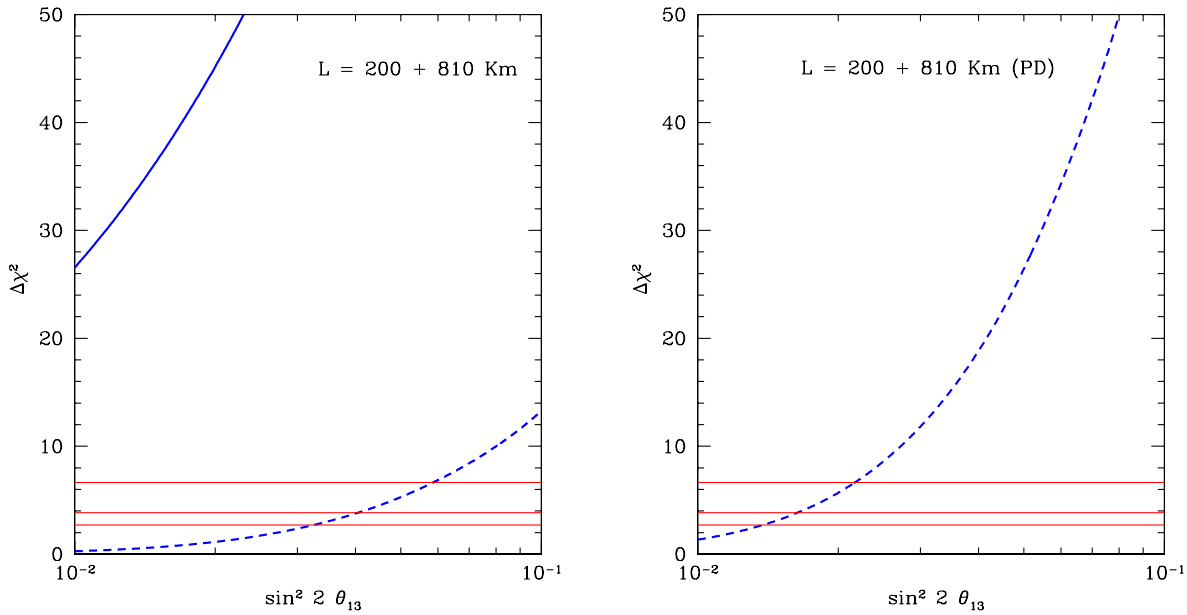

FIG. 6: *(a) Results of the χ^2 analysis to the sign of the atmospheric mass difference extraction versus $\sin^2 2\theta_{13}$, by exploiting the data from a far long-baseline experiment at 810 km and from a short-baseline experiment at 200 km, for $|\Delta m^2_{31}| = 2.4\times10^{-3}$ eV^2. The corresponding 90%, 95% and 99% C.L.s are shown. As a function of $\sin^2 2\theta_{13}$, we depict the maximum (solid line) and minimum (dashed line) of $\Delta\chi^2$, which are obtained for different values of δ depending on $\sin^2 2\theta_{13}$. (b) Same as (a) but with a Proton Driver.*

Driver. This is comparable to what the Super-NOνA setup proposed here can achieve after 5 years of running with only neutrinos and with Proton Driver (see Fig. 5). However, a direct comparison needs to take into account the different choices of detectors, the numbers of protons on target, the value of Δm^2_{31} used in the analysis, and the fact that an optimization of the experiment has not been performed in our case.

We have performed an independent χ^2 analysis of the data on the $\sin^2 2\theta_{13}$–δ plane. At a fixed value for the former two parameters, the χ^2 in the combination of two baselines (near and far sites) reads

$$\chi^2_{\ell\ell'} = \sum_{\ell\ell'} (\mathcal{N}_{\ell,\pm} - N_{\ell,\pm}) C^{-1}_{\ell:\ell'} (\mathcal{N}_{\ell',\pm} - N_{\ell',\pm}) \,, \tag{4.6}$$

where the + (−) sign refers to normal (inverted) hierarchy and C is the covariance matrix, which for the particular analysis considered in the present study contains only statistical errors. The experimental "data", $\mathcal{N}_{\ell,\pm}$, are given by

$$\mathcal{N}_{\ell,\pm} = \langle N_{\ell,\pm} + N_{b\ell} \rangle - N_{b\ell,\pm} \,, \tag{4.7}$$

where we have considered that the efficiencies are flat in the visible energy window, $N_{b\ell}$ are the background events and $\langle\rangle$ means a Gaussian/Poisson smearing (according to the statistics). We have assumed that nature has chosen a given sign for Δm^2_{31}, but the data analysis is performed with the opposite sign. We show the results of our χ^2 analysis in Fig. 6, where we plot the sensitivity to $sign(\Delta m^2_{31})$ after the combination of the data from the long-baseline (810 km) with the data from a short baseline at 200 km. For every value of $\sin^2 2\theta_{13}$ we find the two values[9] of δ that maximize and minimize $\Delta\chi^2$. We depict in Fig. 6 the value of the minimum and maximum $\Delta\chi^2$ versus $\sin^2 2\theta_{13}$. If $\sin^2 2\theta_{13} \geq 0.04$ a misidentification in the sign of the atmospheric mass difference can be excluded at 95% C.L. in the most pessimistic situation. There exists, however, a large number of values of δ at which this misidentification can be excluded at a confidence level larger that 99%. With a proton driver, if $\sin^2 2\theta_{13} \geq 0.02$, our analysis shows that it is possible to determine $sign(\Delta m^2_{31})$ at the level of the 99% C.L. for the full range of δ. The results from the χ^2 analysis presented here agree with the previous study of the asymmetries.

[9] The values of δ at the maximum and minimum of $\Delta\chi^2$ are in general different for different values of $\sin^2 2\theta_{13}$.

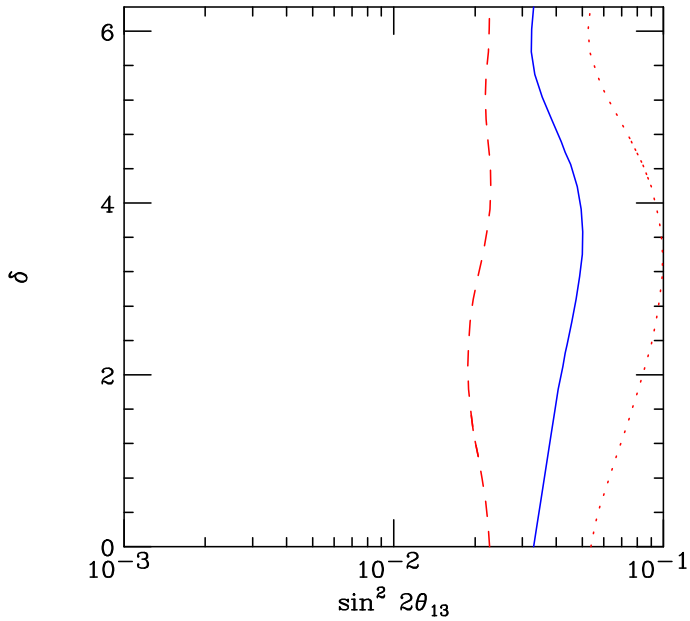

FIG. 7: *Sensitivity to the sign of the atmospheric mass square difference as defined in Eq. (4.5), for different values of* $|\Delta m^2_{31}| = 2.0 \times 10^{-3}$ eV^2 *(dotted red line),* 2.4×10^{-3} eV^2 *(solid blue line), and* 3.0×10^{-3} eV^2 *(dashed red line). We have included the systematic errors induced by the uncertainties on the atmospheric mixing parameters and on the matter parameter A, and exploited the data from a short-baseline off-axis detector located at 200 km and from the long-baseline off-axis detector at 810 km. The experimental setup assumed to perform the solid curves is* 3.7×10^{20} *protons on target per year, a 50 kton detector with perfect efficiencies at each location, and five years of data taking.*

A. Dependence on $|\Delta m^2_{31}|$

In the previous section, we have assumed the knowledge of $|\Delta m^2_{31}|$ with a 5% uncertainty. In particular, we have taken $|\Delta m^2_{31}| = (2.40 \pm 0.12) \times 10^{-3}$ eV^2. Although the former level of precision is expected to be achieved by the time this experiment could turn on [40, 74], currently the value of the atmospheric mass difference is not known with that level of accuracy. Thus, it is important to investigate how the results presented above change if $|\Delta m^2_{31}|$ happens to be different from the previously assumed value.

In Fig. 7 we have depicted the sensitivity to the sign of the atmospheric mass square difference determination as defined in Eq. (4.5), for three different possibilities for its absolute value, $|\Delta m^2_{31}| = 2.0 \times 10^{-3}$eV^2 (dotted red line); 2.4×10^{-3}eV^2 (solid blue line) and 3.0×10^{-3}eV^2 (dashed red line). We have assumed a near off-axis detector located at 200 km. As can be seen from the figure, the larger the value of $|\Delta m^2_{31}|$, the better the sensitivity to the type of neutrino mass hierarchy. The reason can be easily understood from Eq. (4.2). The asymmetry depends on the factor $1/x - 1/\tan x$, where $x \propto \Delta m^2_{31}$ (recall that L/E is the same for both detectors). This function increases monotonically as x increases, and therefore the asymmetry is larger for larger $|\Delta m^2_{31}|$, which correspondingly means better sensitivity.

On the other hand, it must be remarked that since the CHOOZ [13] bound is weaker for small values of $|\Delta m^2_{31}|$, the loss in range for θ_{13} is not as large as one would naïvely think from Fig. 7.

In case the actual value of $|\Delta m^2_{31}|$ happens to be in the low side of the currently allowed range [7], a possible solution could be to adopt a larger L/E, which can be accomplished either by considering longer baselines or larger off-axis angles, i.e., smaller energies. However, both possibilities imply the reduction of the flux at the detectors, so a compromise must be achieved. Nevertheless, if θ_{13} is very small and $|\Delta m^2_{31}|$ is also small, then a longer run in the neutrino mode would unavoidably be needed in order to increase the statistics. All in all, a detailed analysis would be required to find the best possible configuration as a function of $|\Delta m^2_{31}|$ [73].

V. CONCLUSIONS

Establishing the type of neutrino mass hierarchy — be it normal or inverted — plays a crucial role in our understanding of neutrino physics. Future long-baseline experiments will address this fundamental question. Typically the determination of the hierarchy in the proposed experiments suffers from degeneracies with other CP–conserving and CP–violating parameters, namely θ_{13}, δ and θ_{23}. Resolving such degeneracies in one experiment is very challenging, if not impossible. Different strategies have been studied, e. g., by combining more than one experiment [59, 60, 61, 62, 63, 65], using more than one detector [51, 55, 56, 57, 58], or using additional information from atmospheric neutrino data [64].

In the present article, we have presented a method for establishing $sign(\Delta m^2_{31})$, free of degeneracies, by using only one experiment running in the neutrino mode alone. We have considered an experimental setup with two neutrino detectors placed in a special off-axis configuration. It is known that off-axis spectra are well peaked at a certain neutrino energy, which depends on the angle from the central axis of the beam. This allows both detectors to be located in such a way that they have the same L/E. We have shown that very interesting synergy effects show up with this special configuration for which vacuum oscillation phases are the same at both sites, stressing the different matter effects. These are manifest when comparing the bi–event neutrino–neutrino (Fig. 3) and bi–event neutrino–antineutrino (Fig. 4) plots above, for which a clear distinction of the type of hierarchy is possible for the former regardless of the value of δ, but more challenging for the latter.

We have considered a normalized difference, $\mathcal{D}$ (see Eq. (4.1)), between the neutrino oscillation probabilities at two baselines. At leading order, the sign of $\mathcal{D}$ depends only on matter effects, i. e., on the type of neutrino mass hierarchy, while other parameters are subdominant. Although CP–violating terms can have a sizable contribution for small values of $\sin^2 2\theta_{13}$, they cannot change the sign of $\mathcal{D}$. This implies that the determination of the type of hierarchy, exploiting the method discussed here, suffers no degeneracies from other parameters. We have confirmed such a result by performing an analysis of the sensitivity to the mass hierarchy in a specific experimental setup, which we have named Super-NOνA. We propose to use the NuMI beam in the neutrino mode and two detectors, one at the far distance proposed by the NOνA Collaboration, $L_{\rm F} \sim 800$ km, and the other with a shorter baseline, $L_{\rm N} \sim 200$ km (434 km), with the energy tunned to $E_{\rm N} = E_{\rm F} L_{\rm N}/L_{\rm F}$. The selection of the short baseline must be done in such a way that it is possible to place a detector at the precise off-axis angle, in order to get that particular energy at the peak of the spectrum. Because of the Earth curvature, the near detector, located on the Earth surface and on the vertical of the on-axis beam, is off-axis by a small angle, which is the minimum possible off-axis angle at that distance. This implies that not all different configurations, such that L/E is the same at both sites, are possible. In particular, there are no sites between 300 and 400 km which give an L/E ratio of 352 km/GeV.

By considering the integrated asymmetry, Eq. (4.4), we have shown that a suitable baseline for the second detector to determine the type of neutrino mass hierarchy corresponds to $L_{\rm N} \sim 200$ km, which enhances matter effects without the need of too low energies to keep the same L/E at both detectors. We have shown in Figs. 5 and 6 that this can be achieved at 95% C.L., regardless of the value of δ, for $\sin^2 2\theta_{13} \geq 0.05$ for a conventional beam and for $\sin^2 2\theta_{13} \geq 0.02$ with a Proton Driver. Similar results can be obtained for a slightly longer baseline, e. g., 434 km. We have also performed an independent χ^2 analysis of the simulated data on the $\sin^2 2\theta_{13}$–δ plane, which confirms our previous results. This is in contrast with the sensitivity of the proposed NOνA experiment. At the 95% C.L., only for 10% of the values of the CP–phase δ, NOνA can resolve the type of neutrino mass hierarchy if $\sin^2 2\theta_{13} = 0.04$, considering three years of neutrino plus three years of antineutrino running [40, 41].

In Fig. 7 we have also shown the sensitivity to the type of neutrino mass hierarchy for three values of $|\Delta m^2_{31}|$ for the adopted configuration, and as can be seen from it, if $|\Delta m^2_{31}|$ lies in the low side of the presently allowed range [7], another configuration [73] or more statistics might be needed.

For our simulations we have considered two 50 kton liquid argon detectors. In addition to the off-axis experiment detailed here (and in general, to any long-baseline neutrino experiment), the physics potential of liquid argon detectors is remarkable. They can also be used as supernova neutrino detectors, for proton-decay searches, and for studies of neutrinoless double beta decay (see Ref. [72] and references therein).

It is important to notice that the use of the neutrino mode alone would allow a reduction of the number of years of data taking if compared with the standard approach of running in the neutrino and then antineutrino modes. In addition, having two identical detectors and only one beam reduces the systematic uncertainties.

Thus, we have presented an improved off-axis experiment with respect to the proposed NOνA experiment with a high sensitivity to the type of neutrino mass hierarchy (free of degeneracies) even with only a neutrino run. The improved capabilities for measuring the value of θ_{13} and the CP–violating phase, as well as other possible configurations, will be studied elsewhere [73].

VI. ACKNOWLEDGMENTS

We are indebted to Mark Messier and Adam Para for providing us with information about the off-axis neutrino fluxes and to André de Gouvêa and Stefano Rigolin for a careful reading of the manuscript. OM would like to thank Stephen Parke for enlightening suggestions about this work. SP would also like to thank Maurizio Piai for stimulating discussions at the early stages of this work. Our calculations made extensive use of the Fermilab General-Purpose Computing Farms [76]. SPR is supported by NASA Grant ATP02-0000-0151 and by the Spanish Grant FPA2002-00612 of the MCT. Fermilab is operated by URA under DOE contract DE-AC02-76CH03000.

APPENDIX A

We present in this appendix the computed charged-current neutrino event rates for the NuMI beam and different locations of a 50 kton liquid argon detector. As a matter of illustration, we show these event rates in Tables I, II and III for a given value of $\sin^2 2\theta_{13} = 0.058$, a given value of $|\Delta m^2_{31}| = 2.4 \times 10^{-3}$ eV^2, and for four different values of the CP–phase, $\delta = 0, \pi/2, \pi, 3\pi/2$. In these tables we show the unoscillated ν_μ-like events, the expected oscillated ν_e-like signal and the ν_e intrinsic background, which mainly comes from μ decays.

$\sin^2 2\theta_{13}$	δ	Δm^2_{31} (eV^2)	ν_μ(unoscillated)	ν_e (signal)	ν_e (intrinsic background)
0.058	0	0.0024	16322	481	59
0.058	$\pi/2$	0.0024	16322	526	59
0.058	π	0.0024	16322	367	59
0.058	$3\pi/2$	0.0024	16322	323	59
0.058	0	-0.0024	16322	264	59
0.058	$\pi/2$	-0.0024	16322	398	59
0.058	π	-0.0024	16322	353	59
0.058	$3\pi/2$	-0.0024	16322	219	59

TABLE I: *Calculated charged-current neutrino event rates (signal and backgrounds) for NOνA (baseline of 810 km, 10 km off-axis), for* 3.7×10^{20} *pot/yr, 5 years running at a 50 kton far detector. We have computed them for* $|\Delta m^2_{31}| = 2.4 \times 10^{-3}$ eV^2, $\sin^2 2\theta_{13} = 0.058$ *and four values of* $\delta = 0, \frac{\pi}{2}, \pi, \frac{3\pi}{2}$. *The remaining oscillation parameters are* $\Delta m^2_{21} = 8.0 \times 10^{-5}$ eV^2, $\sin^2\theta_{12} = 0.31$, $\sin^2 2\theta_{23} = 1$ *and the matter parameter* $A \equiv \sqrt{2} G_F n_e = 1.064 \times 10^{-4}$ eV^2/GeV. *The energy window is [1.8,2.8]* GeV. *The neutrino spectrum peaks at 2.3* GeV.

$\sin^2 2\theta_{13}$	δ	Δm^2_{31} (eV^2)	ν_μ(unoscillated)	ν_e (signal)	ν_e (intrinsic background)
0.058	0	0.0024	13285	342	81
0.058	$\pi/2$	0.0024	13285	373	81
0.058	π	0.0024	13285	257	81
0.058	$3\pi/2$	0.0024	13285	226	81
0.058	0	-0.0024	13285	228	81
0.058	$\pi/2$	-0.0024	13285	335	81
0.058	π	-0.0024	13285	301	81
0.058	$3\pi/2$	-0.0024	13285	193	81

TABLE II: *Same as Table I for a baseline of 434 km (10.23 km off-axis). The matter parameter* $A \equiv \sqrt{2} G_F n_e = 8.93 \times 10^{-5}$ eV^2/GeV, *and the energy window is [0.8,1.8]* GeV. *The neutrino spectrum peaks at 1.3* GeV.

$\sin^2 2\theta_{13}$	δ	Δm^2_{31} (eV^2)	ν_μ(unoscillated)	ν_e (signal)	ν_e (intrinsic background)
0.058	0	0.0024	8253	163	83
0.058	$\pi/2$	0.0024	8253	177	83
0.058	π	0.0024	8253	122	83
0.058	$3\pi/2$	0.0024	8253	108	83
0.058	0	-0.0024	8253	123	83
0.058	$\pi/2$	-0.0024	8253	177	83
0.058	π	-0.0024	8253	160	83
0.058	$3\pi/2$	-0.0024	8253	106	83

TABLE III: *Same as Table I for a baseline of 200 km (8.44 km off-axis). The matter parameter* $A \equiv \sqrt{2}G_F n_e = 3.83 \times 10^{-5}$ eV^2/GeV*, and the energy window is [0.2,1.2]* GeV*. The neutrino spectrum peaks at 0.7* GeV*.*

[1] B. T. Cleveland *et al.*, Astrophys. J. **496**, 505 (1998);
Y. Fukuda *et al.* [Kamiokande Collaboration], Phys. Rev. Lett. **77**, 1683 (1996);
J. N. Abdurashitov *et al.* [SAGE Collaboration], J. Exp. Theor. Phys. **95**, 181 (2002);
W. Hampel *et al.* [GALLEX Collaboration], Phys. Lett. B **447**, 127 (1999);
T. A. Kirsten [GNO Collaboration], Nucl. Phys. Proc. Suppl. **118**, 33 (2003).
[2] S. Fukuda *et al.* [Super-Kamiokande Collaboration], Phys. Lett. B **539**, 179 (2002).
[3] Q. R. Ahmad *et al.* [SNO Collaboration], Phys. Rev. Lett. **87**, 071301 (2001).
[4] Q. R. Ahmad *et al.*, Phys. Rev. Lett. **89**, 011301 (2002) and *ibid.* **89**, 011302 (2002).
[5] S. N. Ahmed *et al.* [SNO Collaboration], Phys. Rev. Lett. **92**, 181301 (2004).
[6] B. Aharmim *et al.* [SNO Collaboration], nucl-ex/0502021.
[7] Y. Ashie *et al.* [Super-Kamiokande Collaboration], hep-ex/0501064.
[8] K. Eguchi *et al.* [KamLAND Collaboration], Phys. Rev. Lett. **90**, 021802 (2003).
[9] E. Aliu *et al.* [K2K Collaboration], Phys. Rev. Lett. **94**, 081802 (2005);
M. H. Ahn *et al.* [K2K Collaboration], Phys. Rev. Lett. **90**, 041801 (2003).
[10] A. Aguilar *et al.* [LSND Collaboration], Phys. Rev. D **64**, 112007 (2001).
[11] G. Barenboim *et al.*, JHEP **0210**, 001 (2002);
G. Gelmini, S. Palomares-Ruiz and S. Pascoli, Phys. Rev. Lett. **93**, 081302 (2004).
[12] A. A. Aguilar-Arevalo *et al.* [MiniBooNE Collaboration], The MiniBooNE Run Plan, available at `http://www-boone.fnal.gov/publicpages/runplan.ps.gz`
[13] M. Apollonio *et al.*, Phys. Lett. B **466**, 415 (1999).
[14] F. Boehm *et al.*, Phys. Rev. Lett. **84**, 3764 (2000) and Phys. Rev. D **62**, 072002 (2000).
[15] Y. Ashie *et al.* [Super-Kamiokande Collaboration], Phys. Rev. Lett. **93**, 101801 (2004).
[16] T. Araki *et al.* [KamLAND Collaboration], Phys. Rev. Lett. **94**, 081801 (2005).
[17] V. N. Gribov and B. Pontecorvo, Phys. Lett. **B28**, 493 (1969).
[18] M. C. Gonzalez-Garcia, hep-ph/0410030.
[19] M. Maltoni *et al.*, New J. Phys. **6**, 122 (2004).
[20] E. Ables *et al.* [MINOS Collaboration], FERMILAB-PROPOSAL-0875.
[21] M. Guler *et al.* [OPERA Collaboration], CERN-SPSC-2000-028.
[22] P. Aprili *et al.* [ICARUS Collaboration], CERN-SPSC-2002-027.
[23] H. Back *et al.*, hep-ex/0412016.
[24] B. Pontecorvo, Sov. Phys. JETP **6**, 429 (1957) [Zh. Eksp. Teor. Fiz. **33**, 549 (1957)] and *ibid.* **7**, 172 (1958) [*ibid.* **34** (1958) 247];
Z. Maki, M. Nakagawa and S. Sakata, Prog. Theor. Phys. **28**, 870 (1962).
[25] A. De Rújula, M. B. Gavela and P. Hernández, Nucl. Phys. B **547**, 21 (1999);
V. Barger *et al.*, Phys. Rev. D **62**, 013004 (2000);
M. Freund *et al.*, Nucl. Phys. B **578**, 27 (2000).
[26] A. Cervera *et al.*, Nucl. Phys. B **579**, 17 (2000) [Erratum-*ibid.* B **593**, 731 (2001)].
[27] P. Zucchelli, Phys. Lett. B **532**, 166 (2002).
[28] M. Mezzetto, J. Phys. G **29**, 1781 (2003) and *ibid.* **29** 1771 (2003).
[29] For a recent study of the optimal β-beam at the CERN-SPS, see: J. Burguet-Castell *et al.*, hep-ph/0503021.
[30] J. Burguet-Castell *et al.*, Nucl. Phys. B **695**, 217 (2004).
[31] S. T. Petcov, Phys. Lett. B **434**, 321 (1998) [Erratum-*ibid.* B **444** 584 (1998)];
E. K. Akhmedov, Nucl. Phys. B **538**, 25 (1999);

M. V. Chizhov, M. Maris and S. T. Petcov, hep-ph/9810501;
M. V. Chizhov and S.T. Petcov, Phys. Rev. Lett. **83**, 1096 (1999); *ibid.* **85**, 3979 (2000) and Phys. Rev. D **63**, 073003 (2001).
[32] M. C. Bañuls, G. Barenboim and J. Bernabéu, Phys. Lett. B **513**, 391 (2001);
J. Bernabéu and S. Palomares-Ruiz, hep-ph/0112002, and Nucl. Phys. Proc. Suppl. **110**, 339 (2002).
[33] J. Bernabéu *et al.*, Phys. Lett. B **531**, 90 (2002);
S. Palomares-Ruiz and J. Bernabéu, Nucl. Phys. Proc. Suppl. **138**, 398 (2005).
[34] J. Bernabéu, S. Palomares Ruiz and S. T. Petcov, Nucl. Phys. B **669**, 255 (2003);
S. Palomares-Ruiz and S. T. Petcov, Nucl. Phys. B **712**, 392 (2005);
S. T. Petcov and S. Palomares-Ruiz, hep-ph/0406106.
[35] E. K. Akhmedov *et al.*, Nucl. Phys. B **542**, 3 (1999);
D. Indumathi and M. V. N. Murthy, Phys. Rev. D **71**, 013001 (2005);
R. Gandhi *et al.*, hep-ph/0411252.
[36] C. Lunardini and A. Y. Smirnov, Nucl. Phys. B **616**, 307 (2001) and JCAP **0306**, 009 (2003);
K. Takahashi and K. Sato, Phys. Rev. D **66**, 033006 (2002) and Prog. Theor. Phys. **109**, 919 (2003);
A. S. Dighe, M. T. Keil and G. G. Raffelt, JCAP **0306**, 005 (2003) and *ibid.* **0306**, 006 (2003);
A. S. Dighe *et al.* JCAP **0401**, 004 (2004);
A. Bandyopadhyay *et al.* hep-ph/0312315;
V. Barger, P. Huber and D. Marfatia, hep-ph/0501184.
[37] P. I. Krastev and S. T. Petcov, Phys. Lett. B **205**, 84 (1988);
J. Arafune and J. Sato, Phys. Rev. D **55**, 1653 (1997);
J. Bernabéu, Proc. WIN'99, World Scientific (2000), p. 227, hep-ph/9904474;
M. Freund, M. Lindner and A. Romanino, Nucl. Phys. B **562**, 29 (1999);
J. Bernabéu and M. C. Bañuls, Nucl. Phys. Proc. Suppl. **87** (2000) 315.
[38] K. Anderson *et al.*, hep-ex/0402041;
F. Ardellier *et al.*, hep-ex/0405032.
[39] Y. Hayato *et al.*, Letter of Intent, available at `http://neutrino.kek.jp/jhfnu/`
[40] I. Ambats *et al.* [NOvA Collaboration], FERMILAB-PROPOSAL-0929, March 15, 2004, available at `http://www-nova.fnal.gov/reports_page.html`
[41] I. Ambats *et al.* [NOvA Collaboration], hep-ex/0503053. FERMILAB-PROPOSAL-0929, March 21, 2005. Revised NOνA Proposal available at `http://www-nova.fnal.gov/NOvA_Proposal/Revised_NOvA_Proposal.html`
[42] S. Pascoli, S. T. Petcov and W. Rodejohann, Phys. Lett. B **558**, 141 (2003).
[43] S. M. Bilenky *et al.* Phys. Lett. B **465**, 193 (1999).
[44] S. M. Bilenky, S. Pascoli and S. T. Petcov, Phys. Rev. D **64**, 053010 (2001);
S. Pascoli and S. T. Petcov, Phys. Lett. B **544**, 239 (2002) and *ibid.* B **580**, 280 (2004).
[45] S. M. Bilenky and C. Giunti, hep-ph/9904328;
F. Vissani, JHEP **9906**, 022 (1999);
M. Czakon, J. Gluza and M. Zralek, hep-ph/0003161;
H. V. Klapdor-Kleingrothaus, H. Paes and A. Yu. Smirnov, Phys. Rev. D **63**, 073005 (2001).
[46] S. Pascoli, S. T. Petcov and L. Wolfenstein, Phys. Lett. B **524**, 319 (2002);
S. Pascoli and S. T. Petcov, Phys. Atom. Nucl. **66**, 444 (2003) [Yad. Fiz. **66**, 472 (2003)].
[47] S. Pascoli, S. T. Petcov and W. Rodejohann, Phys. Lett. B **549**, 177 (2002).
[48] S. M. Bilenky *et al.* Phys. Rev. D **54**, 4432 (1996).
[49] W. Rodejohann, Nucl. Phys. B **597**, 110 (2001);
K. Matsuda, N. Takeda, T. Fukuyama and H. Nishiura, Phys. Rev. D **62**, 093001 (2000);
H. Nunokawa, W. J. C. Teves and R. Zukanovich Funchal, Phys. Rev. D **66**, 093010 (2002).
[50] G. L. Fogli and E. Lisi, Phys. Rev. D **54**, 3667 (1996).
[51] J. Burguet-Castell *et al.* Nucl. Phys. B **608**, 301 (2001).
[52] H. Minakata and H. Nunokawa, JHEP **0110**, 001 (2001).
[53] V. Barger, D. Marfatia and K. Whisnant, Phys. Rev. D **65**, 073023 (2002);
[54] T. Kajita, H. Minakata and H. Nunokawa, Phys. Lett. B **528**, 245 (2002);
H. Minakata, H. Nunokawa and S. J. Parke, Phys. Rev. D **66**, 093012 (2002);
M. Freund, P. Huber and M. Lindner, Nucl. Phys. B **615**, 331 (2001);
P. Huber, M. Lindner and W. Winter, Nucl. Phys. B **645**, 3 (2002);
A. Donini, D. Meloni and S. Rigolin, JHEP **0406**, 011 (2004);
M. Aoki, K. Hagiwara and N. Okamura, hep-ph/0311324;
O. Yasuda, New J. Phys. **6**, 83 (2004).
[55] D. Beavis *et al.* [E889 Collaboration], Physics Design Report, BNL No. 52459 (April 1995).
[56] H. Minakata and H. Nunokawa, Phys. Lett. B **413**, 369 (1997).
[57] A. Donini, D. Meloni and P. Migliozzi, Nucl. Phys. B **646**, 321 (2002);
D. Autiero *et al.*, Eur. Phys. J. C **33**, 243 (2004).
[58] V. Barger, D. Marfatia and K. Whisnant, Phys. Rev. D **66**, 053007 (2002).
[59] V. Barger, D. Marfatia and K. Whisnant, Phys. Lett. B **560**, 75 (2003).
[60] P. Huber, M. Lindner and W. Winter, Nucl. Phys. B **654**, 3 (2003).

[61] H. Minakata, H. Nunokawa and S. J. Parke, Phys. Rev. D **68**, 013010 (2003).
[62] Y. F. Wang *et al.* [VLBL Study Group H2B-4], Phys. Rev. D **65**, 073021 (2002);
J. Burguet-Castell *et al.*, Nucl. Phys. B **646**, 301 (2002);
K. Whisnant, J. M. Yang and B. L. Young, Phys. Rev. D **67**, 013004 (2003);
P. Huber *et al.*, Nucl. Phys. B **665**, 487 (2003);
P. Huber *et al.*, Phys. Rev. D **70**, 073014 (2004);
A. Donini *et al.*, Nucl. Phys. B **710**, 402 (2005);
A. Donini, E. Fernández-Martínez and S. Rigolin, hep-ph/0411402.
[63] O. Mena and S. J. Parke, Phys. Rev. D **70**, 093011 (2004).
[64] P. Huber, M. Maltoni and T. Schwetz, hep-ph/0501037.
[65] O. Mena, Mod. Phys. Lett. A **20**, 1 (2005).
[66] A. de Gouvea, J. Jenkins and B. Kayser, hep-ph/0503079;
H. Nunokawa, S. Parke and R. Z. Funchal, hep-ph/0503283.
[67] J. Cooper has already used this name for the case of two off-axis detectors using the NUMI beam and with Proton Driver. We use the same name, although the location of the second detector is completely different and we study the case with and without Proton Driver. See J. Cooper's talk at the Fermilab Proton Driver Workshop, 6-9 October, 2004, Fermilab, `http://www-td.fnal.gov/projects/PD/PhysicsIncludes/Workshop/index.html`
[68] M. Freund, Phys. Rev. D **64**, 053003 (2001).
[69] A. Para and M. Szleper, hep-ex/0110032.
[70] M. Messier, private communication.
[71] A. Para, private communication.
[72] L. Bartoszek *et al.*, hep-ex/0408121.
[73] O. Mena, S. Palomares-Ruiz and S. Pascoli, in preparation.
[74] M. Messier, "The NOνA experiment", talk presented at *Neutrino 2004*, available at `http://neutrino2004.in2p3.fr/`
[75] R. J. Geller and T. Hara, Nucl. Instrum. Meth. A **503**, 187 (2001);
S. V. Panasyuk, REM (Reference Earth Model) web page, `http://cfauvcs5.harvard.edu/lana/rem/index.htm`
[76] M. Albert *et al.*, "The Fermilab Computing Farms in 2001–2002," FERMILAB-TM-2209l, available at `http://library.fnal.gov/archive/test-tm/2000/fermilab-tm-2209.pdf`